Geophysical Research Letters

Supporting Information for

Diverse electron and ion acceleration characteristics observed over Jupiter's main aurora

B. H. Mauk[1], D. K. Haggerty[1], C. P. Paranicas[1], G. Clark[1], P. Kollmann[1], A. M. Rymer[1], J. M. Peachey[1], S. J. Bolton[2], S. M. Levin[3], A. Adriani[4], F. Allegrini[2,5], F. Bagenal[6], B. Bonfond[7], J. E. P. Connerney[8], R. W. Ebert[2], G. R. Gladstone[2], W. S. Kurth[9], D. J. McComas[10,2], D. Ranquist[6], P. Valek[2]

1. The Johns Hopkins University Applied Physics Laboratory, Laurel, Maryland, USA (Barry.Mauk@jhuapl.edu)
2. Southwest Research Institute, San Antonio, Texas, USA
3. Jet Propulsion Laboratory, Pasadena, California, USA
4. Instituto Nazionale di Astrofisica-Instituo di Astofisica e Planetologia Spaziali, Roma, Italy
5. Physics and Astronomy Department, University of Texas at San Antonio, Texas, USA
6. University of Colorado, Boulder, Colorado, USA
7. Université de Liège, Technologies and Astrophys. Res. Institute, LPAP,, Liège, Belgium
8. NASA Goddard Space Flight Center, Greenbelt, Maryland, USA
9. University of Iowa, Iowa City, Iowa, USA
10. Department of Astrophysical Sciences, Princeton University, Princeton, New Jersey, US

Contents of this file

Introduction

Here we address the response of the Jupiter Energetic particle Detector Instrument (JEDI) on NASA's Juno mission to electron distributions that are extreme in various ways (energy, intensity, angular structure). JEDI is documented in Mauk et al. (2017c). Electrons are measured by JEDI using solid state detectors (SSDs) that are 0.50 mm thick and that are attached on the back to a thick shield of Tungsten-Copper (that can redirect some escaping electron back into the SSDs). The fact that some electrons can fully penetrate and leave the detector causes a distortion in the measured spectra. We have developed a procedure described here to correct the contaminated spectra. This same procedure provides a method of clearly discriminating between sharp features caused by auroral acceleration and sharp features that can be caused by the penetrators. This same procedure also provides a technique for identifying regions of saturation, where the sensor cannot process electron events fast enough to reconstruct the original spectral shapes at the lower energies. We also address the issues of very high energy electrons that penetrate the sides of the sensor volume, and the measurement of very narrow electron angular features.

Text S1.

Here we present the procedure that we use to correct the JEDI-measured electron spectra that are contaminated with high energy foreground electrons that penetrate the detector.

The minimum energy of an electron that can fully penetrate the JEDI SSDs is about 400 keV. Above these energies, the deposited energy is lower than the total energy of the electron if the electron fully penetrates the detector. However, because the electrons scatter within the detector, electron energies much higher than 400 keV can be measured on a statistical probability basis, yielding a lower detection efficiency for these electrons. The drop in efficiency for electrons with energies that exceed the penetration depth of the solid state detector has been determined empirically and is parameterized here as an efficiency.

$$Effpen = 1 - Exp\left[-2\left(\frac{480}{EkeV}\right)^3\right] \qquad (1)$$

where EkeV is the kinetic energy of the incoming electron. The technique for empirically establishing this expression and the expressions that follow was to run the entire procedure described here on many different spectra while the tweaking parameters of the expressions. Success was declared when good fitting results were achieved with a single set of parameters for wide diversity of spectral shapes and intensity values.

Every electron that fully penetrates the detector leaves behind a contribution to the minimum ionizing bump in the spectrum (Figure S1A). The shape of the minimum ionizing feature is insensitive to the shape of the penetrating electron spectrum because the energy deposition per unit distance (the so-called dE/dX function) is very flat at these energies (Zombeck, 2007). But, it is not exactly flat, and there are other details (degree of scattering for penetrating electrons with different energies) that lead to some small dependencies of the minimum ionizing peak to the penetrating spectrum. At this point in the development, we assume that the shape of the minimum ionizing spectrum is universal and unchanging. It has been determined empirically and is parameterized here with the following analytic equation:

$$MIfunc = \frac{Func1\ x\ Func2}{35.47} \qquad (2)$$

where

$$Func1 = \frac{(1 + Tanh[0.1\ (EkeV - 112)])^2}{4}$$

$$Func2 = Exp\left[\frac{-(EkeV - 85)}{60}\right]$$

Here the "35.47" is the normalization factor that makes the area under MIfunc equal to 1 (the reason for this factor will become apparent below). This function does not perfectly reproduce the bump in the observed spectra. For the reasons described above, we find that sometimes the peak of the observed minimum ionizing function is slightly higher or lower than the peak parameterized here.

Our procedure is to use a parameterized functional form for the input energetic electron spectrum. The form that we use is from Mauk and Fox, (2010, for electrons); and Mauk (2015, for ions), which is a kappa distribution normalized with an additional power-law break at higher energies. Note that we use this function only for energies greater than about 78 or 90 keV (spectrum dependent); we leave the points below that energy unchanged since those energies have nothing to do with the effects that we are trying to model. The spectrum has the form:

$$Intensity = \frac{C\ EkeV\ [kT\ (g1+1) + EkeV]^{(-g1-1)}}{\left[1 + \left(\frac{EkeV}{Eo}\right)^{g2}\right]} \qquad (3)$$

where EkeV is energy in keV. Here the free parameters that we must optimize are C, kT, g1, Eo, and g2. The units on the intensity are 1/(cm^2 s sr keV).

In the procedure developed here, we keep a careful accounting of particles that are lost and gained. Every particle that is lost (not counted at its actual energy) because it penetrates the detector shows up as a single particle contribution to the minimum ionizing peak. We therefore must know how many particles are lost, not just within the nominal energy range of JEDI, but to much higher energies as well. We therefore must determine the following integral, where PLost is the number of electrons per time that are not detected close to their actual energy, over the area and solid angle of the instrument.

$$PLost = \int_{Elow}^{Ehigh} Intensity\ x\ (1 - Effpen)\ \ dEkeV \qquad (4)$$

from Elow (any energy that is lower than those that can penetrate the detector; e. g. use 30 keV) to Infinity (or a very large number, Ehigh). *Intensity* (Equation 3) refers to the ambient (not measured) distribution of electrons and describes their number at their actual energy, per time, energy range, detector area and solid angle. Note that if the power law of the high energy tail of the incoming electron distribution at the highest energies (g1 + g2 for Equation 3) becomes small enough (close to the value of 1) then the parameter PLost becomes unconstrained (diverges as one integrates to infinity) and the procedure fails.

The procedure now is to optimize the parameters in Intensity (Equation 3) such that we fit the observed spectrum with the following function:

Fit = Intensity x Effpen + PLost x MIfunc (5)

The factor Effpen removes electrons from their ambient energy within the high energy tail, and the second term adds these electrons into the minimum ionizing feature.

Just as an example, this procedure is easy to implement for single spectra in the software Excel using the Solver subprogram (sample available on request). An example of such an optimization for a highly contaminated spectrum is shown in Figure S1A. Here the individual blue symbols are the original data, the solid blue line is the fit (Equation 5) to the data for energies greater than 78 keV. The red line is the input spectra (Equation 3) that has had its parameters

optimized to yield the best fit of the blue solid line to the data (blue symbols). The final result (shown in Figure S1B) comprises the original data for energies up to about 90 keV, and the reconstructed data using the red line for energy greater than or equal to 78 keV.

There are tricks to obtaining the most robust fits over all energies. Our error function that must be minimized uses the logarithm of the intensity values (Error = Sum[Log(model) – Log(data)]^2]). A robust procedure sometimes requires that the sensitivity of the error function to the various parameters be flattened out. One way of doing that is to rewrite Equation (3) into something like:

$$Intensity = \frac{10^{LC}\ \frac{EkeV}{100}\left(\frac{kT}{100}\ \ (g1+1)+\frac{EkeV}{100}\right)^{(-g1-1)}}{\left(1+\left(\frac{EkeV}{Eo}\right)^{g2}\right)} \qquad (6)$$

Here, the energies have been normalized by an energy parameter (100 in this case) that is contained within the range of energies under consideration, a normalization that reduces the sensitivity of the error function to the g1 parameter. In this version we are also optimizing the log of the normalizing parameter (LC) rather than the normalizing parameter itself (C), thereby increasing the sensitivity of the error function to the normalizing parameter.

Text S2.

Here we discuss the effect of electrons that fully penetrate the JEDI solid state detectors on the calculation of moments of the electron distributions.

An important parameter for addressing the impact of energetic electrons on auroral physics is the energy flux that precipitates down onto the atmosphere. The procedure for calculating this parameter has been described elsewhere (Mauk et al., 2017a). But, an important consideration is how that parameter might be modified by the distortions that arise from the penetrating particles. It turns out that if we do no correction, and just use only the original uncorrected data, we obtain a lower limit to the energy flux for electron energies >30 keV. That is because the electrons that are lost within the higher energy tail (including those above the nominal energy range of JEDI) are all counted, but their energies are reassigned to a lower value, close to 160 keV. Note that the number flux that one would obtain by simply integrating the original uncorrected data will be close to the correct value for >30 keV electrons, since the energy assigned to the particles is not relevant to that parameter, provided they are not assigned an energy lower than JEDI's energy range. Only the small percentage of > 1.2 MeV electrons that are fully stopped within the detector are not counted. Hence a characteristic energy (Ec), defined as the ratio of energy flux to number flux, is also a lower limit, when using uncorrected data.

In order to further constrain the energy flux in an automated way we have, in the panels A of Figures 3 and 4, partially corrected the data by applying the efficiency factor in Equation (1) but not trying to subtract off the minimum ionizing peak. The integral of that partially corrected spectrum yields an upper limit to the energy flux with respect to integration over energy. Both a

lower limit and an upper limit are shown in Figures 3A and 4A, to the extent that the spectra are not saturated (see Section S4).

Text S3.

Here we discuss the procedure for cleanly distinguishing between the sharp spectral feature that is caused by high energy electrons that penetrate the JEDI solid state detectors and the sharp spectral features caused by auroral acceleration.

Figure S1A shows that penetrating electrons give rise to a peaked feature that might potentially be mistaken for coherent auroral acceleration. But, what we have found is that when a true coherent auroral acceleration occurs, it is seldom accompanied by a high energy tail sufficient to give a substantial minimum ionizing peak. The procedure documented in Section S1 can be used to test this premise. Figure S1C shows an example where a strong auroral acceleration feature is present (this is spectrum 5 in Figure 5). Here we have run our procedure but have eliminated the data points between about 130 and 350 keV to see how much of a minimum ionizing peak the high energy tail can produce. The minimum ionizing contamination is the very small bump that represents the difference between the solid blue line and the solid red line. This bump is clearly different from the main peak shown in the unconnected symbols, and therefore, for this case, inconsequential for characterizing the auroral acceleration feature.

Text S4.

Here we discuss a procedure for determining when the JEDI electron sensors become partially saturated by particle intensities that are higher than the instrument can fully process.

Electron events within JEDI are processed by an onboard computer that can process up to about 30,000 events per second. Fast field-programmable gate array (FPGA) based counters, and so-called dead time counters, are used on the ground to renormalize the channel rates, allowing for the proper reconstruction of the electron spectra for rates approaching 10^6 counts per second. For even faster rates, proper reconstruction of the spectral intensities and shapes becomes more difficult. The same procedure, documented in section S1, can be used to identify regions where the intensities are too high to be fully quantified by the JEDI sensor. An example is shown in Figure S1D. Here we have blindly applied our spectra correction procedure, and the procedure clearly fails since the blue curve does not match the blue symbols. The high energy tail of the distribution is demanding that there exist a minimum ionizing bump near 160 keV, but the bump is simply not there. In this case the counts per second summed from all of the channels, nominally corrected for a dead time, sum to 1.4E6, outside the nominal count rate range of the sensors. Electronic pulses within the instrument, stimulated by the individual electron events, are landing on top of each other, and the instrument is not able to correctly bin each event. And more specifically, the energies of the events that are binned are smeared out to some extent, particularly at the lower energies. This process has likely broadened the expected minimum ionizing peak (blue curve in Fig S1D) to the observed distribution (blue symbols).

Note that JEDI was designed to mitigate the problem of saturation should it be determined that a substantial fraction of the main auroral crossings would result in saturation. JEDI SSDs have

both large and small pixels (with only large or small pixels active at any one time for each species, electrons and ions; Mauk et al., 2017c). The saturation documented here occurred with large pixels. Going to small pixels reduces the count rates by about a factor of 12. During Juno's first auroral pass (PJ1) large pixels were used in JEDI190 and small pixels were used in JEDI270. Saturation was not detected during PJ1 and thus the decision was made to utilize large pixels on subsequent orbits (currently completed PJ10 at the time of writing). We may contemplate the use of small pixels for some future orbits.

Text S5.

Here we discuss how to distinguish contamination within the JEDI electron sensors that occurs as a result of electrons that have energies high enough to penetrate the detector shielding.

Electrons with energies high enough to penetrate the JEDI experiment box and detector shielding certainly exist within Jupiter's hard radiation regions. The Appendix of Mauk et al., (2017c) shows the shielding geometry and estimates the energies that can penetrate the side walls (>15 MeV) and the blades that make up the collimator structure (> 10 MeV). Mauk et al. (2017a) identified where such penetrators are important for perijove 1 (PJ1). As documented in Paranicas et al. (2017), the presence of penetrators can be identified in regions close enough to Jupiter, where JEDI resolves the loss cone. The upward loss cones should be empty in the radiation belts unless the detectors are contaminated with side penetrators. Elsewhere and where the external distributions have non-isotropic pitch angle distributions, unnatural patterns emerge in the electron pitch angle distributions whenever side penetrators are playing a role. If signatures of penetrators are found, all JEDI electron spectra during this time (not just the spectra pointing into the loss cone) are contaminated and should not be used. This issue is mostly important when Juno passes the horns of the hard radiation belts. Another indication of the importance of side penetrating electrons can be derived by applying the procedure documented in section S1. Even electrons with energies >15 MeV will contribute to the generation of the minimum ionizing feature. Thus, the procedure places constraints even on electrons with energies sufficient to penetrate the sides of the sensor. Because of uncertainty in which electrons come through the collimator and which through the sides of the sensor, this tool cannot yet be used to quantitatively evaluate just how much side-penetrating contamination exists within the data for general positions.

Text S6.

Here we discuss issues that arise with the JEDI electron measurements when the features that are being observed are more structured in angle than can be resolved by the JEDI fields-of-view.

The instantaneous full-width-at-half-maximum field of view (FOV) of the JEDI electron telescopes is about 9°x17°. The accumulation time for each high rate sampling is about 0.5 seconds, corresponding to about 1/60 of a rotation, or about 6° or rotational motion, roughly in the direction that corresponds to the "17°" dimension in the FOV. There are narrow angular beams that JEDI has observed, particularly in the upward direction over the polar cap (Mauk et al., 2017a; see Figure S2). JEDI does not resolve these beams. JEDI's derived intensities will be low for such beam for two different reasons. First, if one generates pitch angle distributions with resolution elements that are too coarse (e. g. 15 degrees), then some observations will be

included in the field-aligned accumulations that do not have the magnetic field line contained within the FOV at any time during the accumulation. For the very narrow beams, one should utilize pitch angle resolutions as narrow as 4.5 degrees to make sure that any accumulation purporting to be in the field-aligned direction actually includes the field line within the accumulation. For a 30 second accumulation, the somewhat offset configuration of the JEDI viewing often allows resolutions down to 4.5 degrees. But there will also be time gaps. For shorter time accumulations it is rare that viewing down to within 4.5 degrees of the field line can be achieved.

It has turned out to be very fortunate (and also physically significant in a way that we do not yet understand) that the downward going intensities over the main aurora are often much broader in angle than the upward going intensities in some main aurora regions. Various analyses have shown that often one may average over, say, 15 degrees without engendering spin modulation in the downward fluxes. However, for the analysis of any particular period of time, the researcher must perform a number of different experiments with the data to make absolutely sure that there is not an angular sampling problem. Such experiments involve plotting and re-plotting the data using a wide variety of combinations of time resolution and angle resolution to see how the character of the plots changes. For example, do you get a sudden burst of energy flux only at the instance when the pitch angle coverage is particularly complete and not elsewhere?

Missing the field line is only one of the ways that intensities might be in error. The second reason that JEDI intensities of beams are a lower limit is this: when we convert count rates into intensities we assume that the FOV of the instrument is uniformly filled. For narrow beams, such as the upward beams over the poles, the FOV is not filled because JEDI does not resolve the beams. Under this circumstance the intensities and energy fluxes will be lower than they should be. No correction has been applied to the JEDI data to mitigate these occurrences.

Text S7.

Here we discuss the issues that arise with the JEDI electron measurements as a result of electron scattering within the JEDI sensor volume.

One of the driving requirements for the JEDI instrument was to be able to obtain nearly complete pitch angle distributions at every instant of time (0.5 second distributions). Because of the rapid motion of the spacecraft (up to 55 km/s) and the slow rotation of the spacecraft (2 rotations per minute), a multiplicity of simultaneous look directions is required. To obtain the needed number of look directions using limited resources, it was necessary to allow the trajectories of the particles to share a common sensor volume (Mauk et al., 2017c). When electrons enter the sensor volume of JEDI, some of them can hit internal structures within the sensor other than the SSDs. A fraction of those electrons can scatter and find their ways to other SSDs from directions that were not intended with the sensor design. This mechanism limits the contrast that can be seen within highly structured features, such as strongly magnetic field aligned beams. Figure S2 shows some example electron pitch angle distributions (30 – 1000 keV) that reveal the character of scattered component. These are measurements of very narrow, magnetic field-aligned electron beams within Jupiter's polar caps (Mauk et al., 2017a). The left hand plots show that the scattered component exists at something like the percent level. However, an aspect of the response that requires special vigilance is the situation where

the electron beam enters the detector from a direction that is not quite ideal; that is the center of the angular beam does not hit the center of the SSD. Rather, parts of the beam are aimed at structures that are off to the side of the SSD. In these cases the contrast between the measured the beam and the scattered component can be less. For example, the plot on the right of Figure S2 shows a contrast (signal to noise) at the 5-10% level. Such low signal-to-noise situations can happen when JEDI does not angularly resolve the features of interest (see also section S6). Much care must be exercised in analyzing these very narrow features.

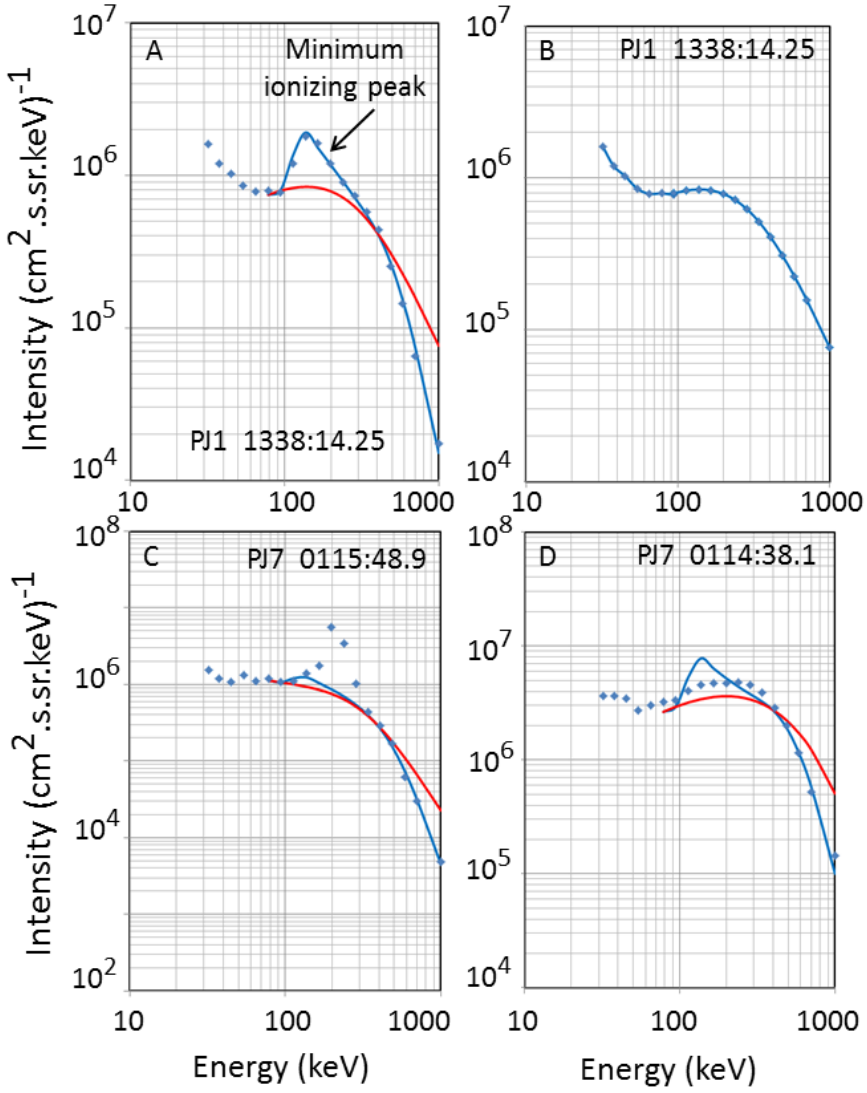

Figure S1. Electron differential number intensity energy spectra sample by the JEDI instrument (blue symbols) used to describe a procedure for correcting the spectra when contaminated by penetrating electrons (panels A and B), testing the degree of such contamination when the detector is seeing coherent auroral acceleration (panel C), and testing whether or not the JEDI sensor is partially saturated (panel D). Blue symbols are the JEDI channel measurements, blue lines are the fits to the measurements (Equation 5) and red lines are the modeled incoming electron spectra (Equation 3). See the text for details.

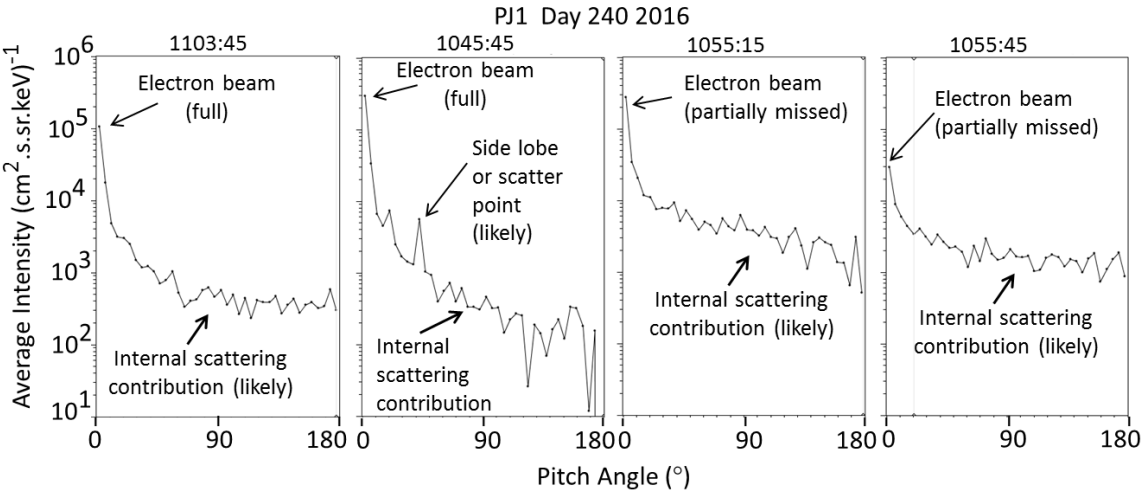

Figure S2. Electron pitch angle distributions measured by JEDI in the polar caps of Jupiter's polar regions where there are extremely narrow, upward going, magnetic field-aligned electron beams (Mauk et al., 2017a). This figure is intended to indicate that, because of internal scattering within the JEDI sensor volume, there are shoulders on the distributions that likely result from internal scattering rather than from electrons entering the sensor from those off-beam directions. These distributions are the energy-averaged differential number intensities, averaged over 30 – 1000 keV.